Thermal and electrical yield of a combi-panel

THERMAL AND ELECTRICAL YIELD OF A COMBI-PANEL

Herman A. Zondag, Douwe W. de Vries and Anton A. van Steenhoven
Department of Mechanical Engineering, Eindhoven University of Technology, P.O.Box 513, 5600 MB Eindhoven, The Netherlands,
Tel.: + 31-40-2472726, fax: + 31-40-2433445, H.A.Zondag@wtb.tue.nl

Wim G.J. van Helden,
Netherlands Energy Research Foundation ECN, P.O. Box 1, 1755 ZG Petten, the Netherlands

Ronald J.C. van Zolingen
Shell Solar Energy BV, P.O. Box 849, 5700 AV Helmond, the Netherlands

Abstract - A first, non-optimised prototype of a combi-panel was built of a PV-laminate and a sheet-and-tube absorber. The thermal efficiency at zero reduced temperature was found to be 54%, along with 8.5% electrical efficiency. The results of the measurements were used to verify the results of the simulations. It was concluded that the simulations and the measurements corresponded sufficiently well. Then, the simulations were used to find the annual efficiency of a PV/T-system that was used for hot-water production in a Dutch household, for which 33% thermal and 6.7% electrical efficiency was found. Finally, the simulations were used to quantify the contribution of the various loss terms to the reduction in thermal efficiency of a PV/T-system with respect to a thermal collector.

1 INTRODUCTION

A combi-panel consists of a PV-laminate that functions as the absorber of a thermal collector. In this way a device is created that converts solar energy into both electrical and thermal energy. The main advantages of combi-panels are:

1. An area covered with combi-panels produces more electrical and thermal energy than a corresponding area partially covered with conventional PV systems and partially filled with conventional thermal collectors. This is particularly useful when the amount of space on a roof is limited. In addition, installation costs are reduced. This will become increasingly important in the future when the price of PV will be reduced.
2. Combi-collectors provide architectural uniformity on a roof, in contrast to a combination of separate PV- and thermal systems.

2 SYSTEM

In order to quantify the efficiency of a PV/T-collector, an experimental prototype was built at the Eindhoven University of Technology. This was a non-optimised first prototype, that was built in order to be able to validate the simulations. The prototype was constructed by connecting a conventional PV-laminate, containing multi-crystalline silicon cells, to the absorber plate of a conventional glass-covered sheet-and-tube collector, as shown in figure 1. The panel was then integrated into a test rig on the roof of the department of Mechanical Engineering at the Eindhoven University of Technology.

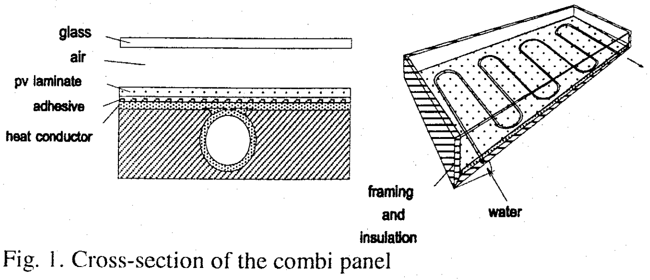

Fig. 1. Cross-section of the combi panel

The efficiency of the combi panel was measured and compared to the efficiencies of a conventional sheet-and-tube-type thermal collector and a multi-crystalline silicon PV-panel of the same length and width, which were positioned next to it in the test rig. A photograph of the test rig is shown in figure 2. The original collector surfaces were somewhat larger than the PV-laminate. In order to create similar areas for the PV laminate, the thermal collector and the combi-panel, the absorbing surfaces of the latter two were partly covered with insulation that had a reflective aluminium top layer. In figure 2 these covered parts appear as the white areas around the collector and the combi-panel. The uncovered parts have an area of 0.94 m^2 each.

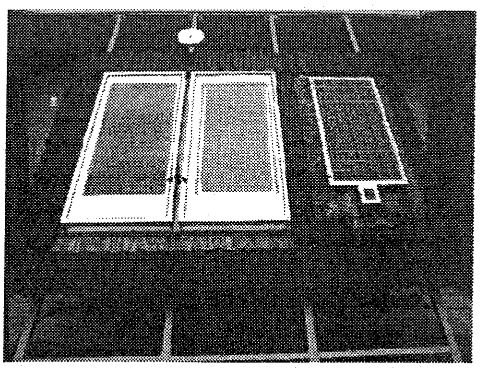

Fig. 2. The test rig. Left to right: a conventional thermal collector, the combi panel and a conventional PV-laminate.

The system consisted further of a water tank of 130 litres. The water was drawn from the tank into the thermal collector and the combi-collector by a NKF Verder ND 300 KT 18 diaphragm pump. The construction was such that the water that was heated by the system could either be returned to the tank or could be discharged on the sewage system in order to keep the water temperature in the tank at a constant value. In the latter case the water level in the tank was kept constant through a tap that was connected to the water supply of the building. The water flow through the combi-panel and the conventional thermal collector were measured independently with two rotary piston KENT PSM-LT PL 10 water volume meters. The volume flow was measured by dividing the counted amount of litres by the measuring time. The wind speed was measured with an EKOPOWER MAXIMUM cup anemometer. The irradiation was measured with a Kipp & Zonen CM 11 pyranometer. The temperatures of the PV-laminate, the combi-panel laminate and the collector absorber as well as the in- and outflow temperatures of the collector and the combi-panel were measured with thermocouples type K which were calibrated to an accuracy of 0.2 K. The thermocouples, the pyranometer, the anemometer, the two water meters and the electrical output of the combi-laminate and the PV-laminate were read out by a DORIC digitrend 220 datalogger. The time between two measurements was typically 11 seconds. The PV laminate was a standard Shell Solar PV-laminate consisting of 72 10×10 cm^2 EVA encapsulated square multi-crystalline silicon cells with a low-iron glass front and an Al/tedlar film at the back. The cell efficiency under STC is typically 13%. The laminate efficiency at 25 ^{0}C is 9.7%.

3 COLLECTOR EFFICIENCY CURVES

3.1 Measurements

The thermal efficiency was measured as a function of reduced temperature. For these measurements, a mass flow of 76 kg/(m^2 hr) was used. The conditions for the measurements were:

1. During a time span of 15 minutes the radiation is at least 750 W/m^2 and its value does not vary more than 100 W/m^2.
2. The fluid inlet temperature and outlet temperature do not vary more than 0.2 K during the measurement.
3. The flow rate for the collector and combi-panel is around 20×10^{-6} m^3/s and varies not more than 1.4×10^{-6} m^3/s.
4. The wind speed during the measurements does not exceed 2 m/s.

In order to check if the restrictions mentioned above are sufficiently strict a set conditions of a somewhat less restrictive nature was applied. It was found that the results did not change significantly.

The thermal efficiency is calculated from quantities averaged over 15 minutes. The thermal efficiency of the combi panel and the thermal efficiency of the conventional collector are presented in figure 3. The electrical efficiency of the combi panel and the PV panel are presented in figure 4.

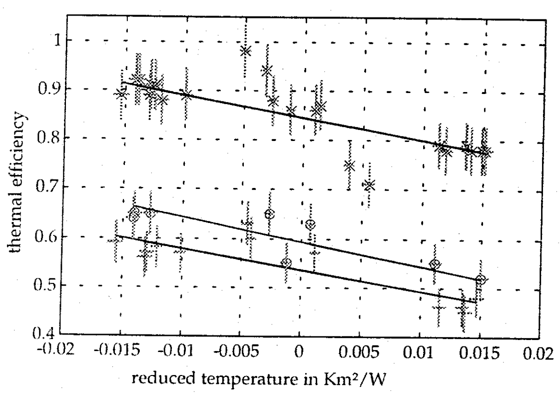

Fig. 3. The thermal efficiency of the thermal collector (×) and the combi-laminate (both with (+) and without (o) electricity production).

Both the electrical yield and the thermal yield are lower than found for the conventional collectors, as expected. However, the results show that two combi-panels together produce more energy per unit area than one PV-laminate and one thermal collector next to each other, which makes them interesting for solar energy production.

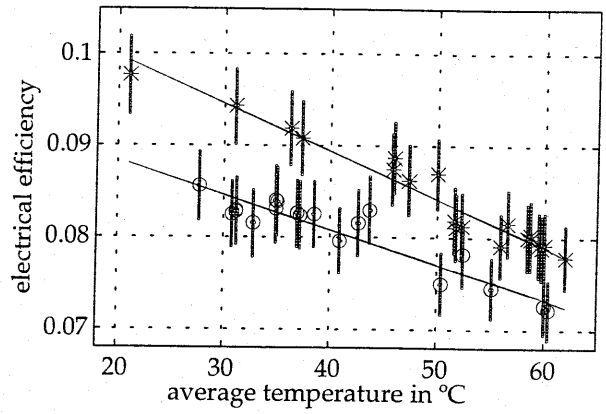

Fig. 4. The electrical efficiency of the PV-laminate (∗) and the combi-laminate (o).

3.2 Simulations

The thermal efficiency is simulated assuming thermal equilibrium in the various layers of the combi-panel and the thermal collector. The relations describing the radiation and convection heat transfer are put in local heat balances for all layers in the combi panel. The sheet and tube type combi-panel is considered as one long straight tube, which implies that symmetry is assumed with respect to the centreline between two successive pipes. The heat flow in the direction perpendicular to the flow direction is calculated with a relation obtained from the well known Hottel-Whillier model for thermal collectors, that is based upon this same assumption of symmetry. It is described extensively by e.g. Duffie and Beckman (1991).

The Hottel-Whillier model leads to a temperature distribution between two tubes in a sheet-and-tube collector that is given by

$$\frac{T(x)-T_{amb}-\tau_{\alpha}I/h_l}{T_b-T_{amb}-\tau_{\alpha}I/h_l}=\frac{\cosh(mx)}{\cosh(m(W-D)/2)} \quad (1)$$

in which τ_α is the transmission-absorption coefficient, I is the irradiation, h_l is the heat loss coefficient, T_{amb} is the ambient temperature and T_b is the temperature at the absorber surface directly above the tube, W is the distance between the tubes and D is the tube diameter. A typical temperature distribution between the collector tubes is shown by figure 5.

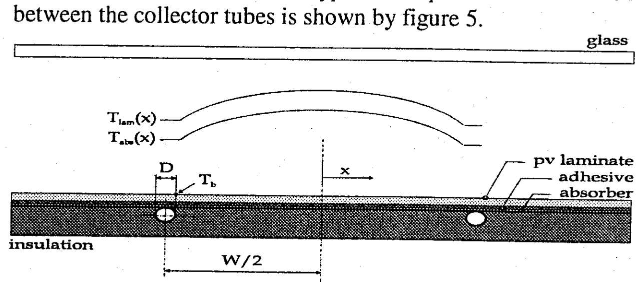

Fig. 5. The temperature profiles of the laminate and the absorber between the tubes of a sheet-and-tube collector.

The coefficient m in formula 1 determines the flatness of the temperature profile and is given by

$$m^2 = \frac{h_l}{\lambda_{Cu}\delta_{Cu}} \quad (2)$$

The temperature gradient across the absorber drives the conductive heat transfer to the collector tubes. At the same time, the high temperature between neighbouring tubes causes additional losses, which means that not all the heat can be collected. This is expressed in the fin efficiency factor F that is given by

$$F = \frac{\tanh(m(W-D)/2)}{m(W-D)/2} \quad (3)$$

For a conventional thermal collector, the heat collection efficiency factor is then defined as

$$F'' = \frac{1/h_l}{W\left(\frac{1}{h_l(D+(W-D)F)} + \frac{\delta_{bond}}{\lambda_{bond}b} + \frac{1}{\pi D h_f}\right)} \quad (4)$$

in which h_l is the heat loss at the top of the laminate and h_f is the heat transfer coefficient to the water in the tubes. The useful energy gain per unit tube length is given by formula 5.

$$q = WF''(\tau_\alpha I - h_l(T_w - T_a)) \quad (5)$$

T_w is the temperature of the water.

In order to account for the special characteristics of the combi-panel, three equations had to be modified with respect to the equations for a conventional thermal collector.

1. Due to conservation of energy, the solar energy that is converted to electricity cannot be converted to thermal energy anymore. Therefore, in the heat equations, τ_α should be replaced by its effective value.

$$\tau_{\alpha,eff} = \tau\left(\frac{\tau_\alpha}{\tau} - \eta_{el}\left(1 - 0.005\left(T_{lam} - 25^0 C\right)\right)\right) \quad (6)$$

2. For τ_α a value of 0.744 was found from a simulation of the optical characteristics of the PV laminate. For the transmission of the glass cover τ a value of 0.92 was applied, based on general low-iron glass transmission data.
3. In the equation for m an additional term appears, due to the fact that the silicon cells provide a parallel channel for heat conduction, along with the conduction sideways through the copper absorber plate.

$$m^2 = \frac{h_l}{\lambda_{Si}\delta_{Si} + \lambda_{Cu}\delta_{Cu}} \quad (7)$$

Only the effects of the silicon and the copper are expressed in the equation, since the heat conduction through the EVA and the glass are much smaller than these. If the heat conduction through the silicon is large, the temperature profile across the combi laminate will be flatter than if the heat conduction is small.

4. In the equation for the heat collection efficiency, an additional term appears due to the heat resistance h_{ca} between cells and absorber. The bond conductance can be neglected due to the high silver content of the bond

$$F'' = \frac{1/h_l}{W\left(\frac{1}{h_l(D+(W-D)F)} + \frac{1}{\pi D h_f} + \frac{1}{W h_{ca}}\right)} \quad (8)$$

F is the fin efficiency factor and h_{ca} is the heat transfer coefficient between the cells and the absorber. If h_{ca} is small, the temperature gradient between the laminate and the copper absorber will be large and a large heat loss to the ambient will occur, which will reduce the thermal efficiency.

5. Finally, a PV-laminate is not spectrally selective, so the emission coefficient was changed from 0.12, which is a typical value for a spectrally selective surface (e.g. Duffie and Beckman (1991)), to 0.9.

The full set of equations provides a matrix, which was solved by a matrix solving procedure of MATLAB. This results in a set of efficiency curves. In figure 6 the calculated efficiency curves are presented together with a least-squares fit of the measurements that were presented previously in figure 3.

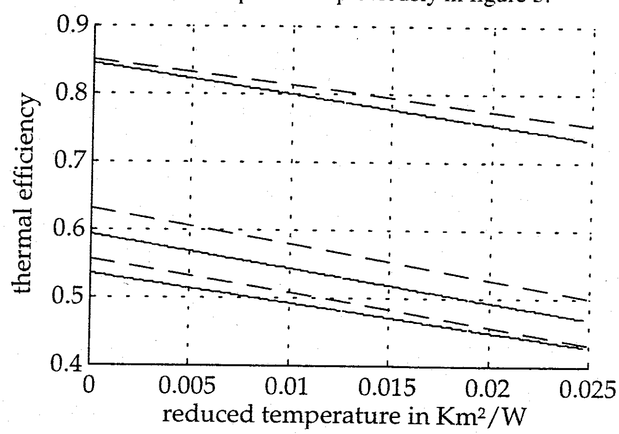

Fig. 6. The simulations of the thermal efficiency (dashed) compared to the least squares fit of the measurements (solid) for a conventional thermal collector and a combi-panel either or not producing electricity.

The figure shows a reasonably good agreement between the simulations and the measurements, although the difference between the curves is in the range 0%-4%, which is somewhat larger than the experimental inaccuracy, which was found to be around 1%. The differences still present might be due to a slight overestimation of the optical efficiency or to heat loss to the sides of the copper absorber (the parts which are covered by insulation in order to keep the area of the PV laminate and the combi absorber-plate equal; see figure 2). In addition, the sky temperature was not measured. In the simulations, it was assumed to be equal to the value for a clear sky. This could also account for a part of the difference. The clear-sky temperature is calculated from the formula

$$T_{sky} = 0.0552 T_{amb}^{1.5} \quad (9)$$

3.3 Estimating the loss terms

Next, the simulations were used to obtain information about the loss mechanisms in a combi-panel. Figure 7 shows the magnitude of the radiation loss, the convection loss and the back loss. Together with these losses, the thermal and the electrical efficiencies are indicated. Finally, the straight line on top is the sum of all these terms, which is equal to the transmission-absorption coefficient of the combi-panel, as expected. The calculation was done by setting T_{amb} = 20 ^{0}C and I = 800 W/m^2 and increasing the inflow temperature, which is of some importance because these settings determine the PV-laminate temperature, which determines the electrical efficiency and which is by itself not a function of reduced temperature. The relative magnitude of the radiation and convection losses depends on the sky temperature. The calculation was done for a clear sky using formula 9.

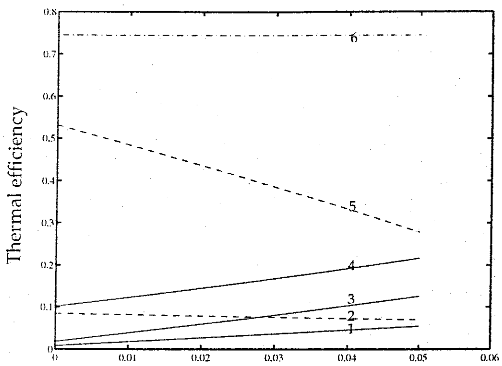

Fig. 7. The loss mechanisms in the combi-panel as a function of reduced temperature (solid lines); (1) back loss, (3) convection loss and (4) radiation loss. The dashed lines indicate the electrical efficiency (2) and the thermal efficiency (5). The dash-dot line (6) represents the sum of all these terms, and is therefore equal to τ_α.

With respect to the reduction in the thermal efficiency of the PV/T-system in comparison to the conventional thermal absorber, simulations were performed in which the special features of the PV/T collector were successively left out. These features are

1. A lower optical efficiency of 0.744 for the PV laminate applied in the first prototype, instead of 0.89 for a conventional thermal absorber. This is particularly important for long-wavelength irradiation
2. A smaller heat transfer between the absorber (the PV laminate) and the water, as indicated by formula 8 (see above). The value of h_{ca} that was found from measuring the temperature difference across the combi-absorber, was approximately 45 W/m^{2}K. Due to this heat resistance, the absorber surface is relatively hot and therefore thermal losses are enhanced.
3. The PV-laminate is not spectrally selective, since glass has a high emission factor in the infrared. This changes the emission of the absorber from 0.12 (for a spectrally selective absorber) to 0.9. This strongly increases radiation losses from the absorbing surface.
4. Due to the additional heat transfer sideways through the silicon (which provides a thermal path parallel to the copper absorber), the heat loss from the collector surface was slightly reduced. However, this effect is very small.
5. Due to conservation of energy, electrical energy can only be produced at the expense of thermal energy.

The effect of these features on the efficiency curves is indicated in figure 8. Particularly the spectrally selective layer seems to have a substantial effect on the slope of the thermal efficiency curve.

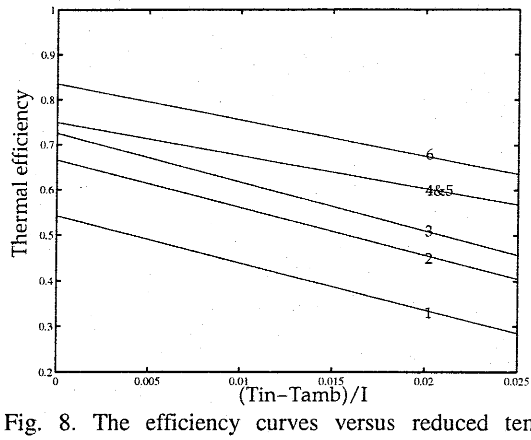

Fig. 8. The efficiency curves versus reduced temperature, successively removing the special features of the combi-panel. From low to high: (1) combi-panel, (2) optical efficiency enhanced, (3) heat transfer enhanced, (4) spectral selectivity enhanced, (5) heat conduction sideways through silicon removed, (6) no electricity produced.

4 SYSTEM EFFICIENCY

4.1 Daily yield

The thermal yield was simulated as a function of reduced temperature by assuming that at each moment the panel is in thermal equilibrium. In these simulations, the top loss was calculated from the empirical formula found by Klein (Duffie and Beckman, 1991, p. 260). In order to test the software program, the daily yield was measured and subsequently simulated. The ambient conditions during the day were those presented in figure 9. The inlet temperature was kept constant.

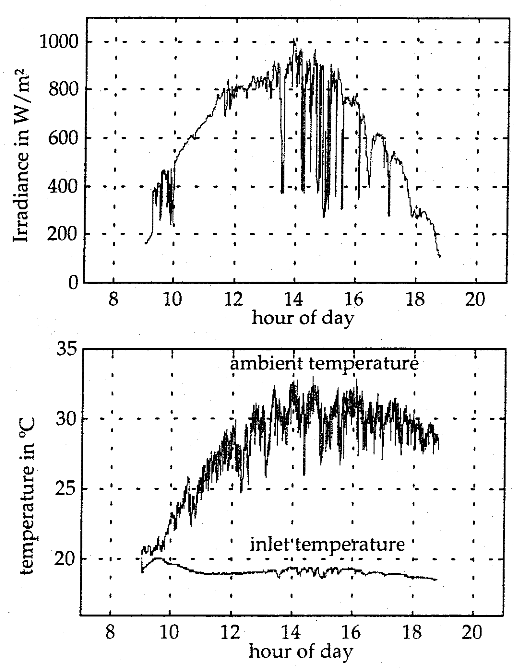

Fig. 9. Ambient conditions on July 12, 1997, against the hour.

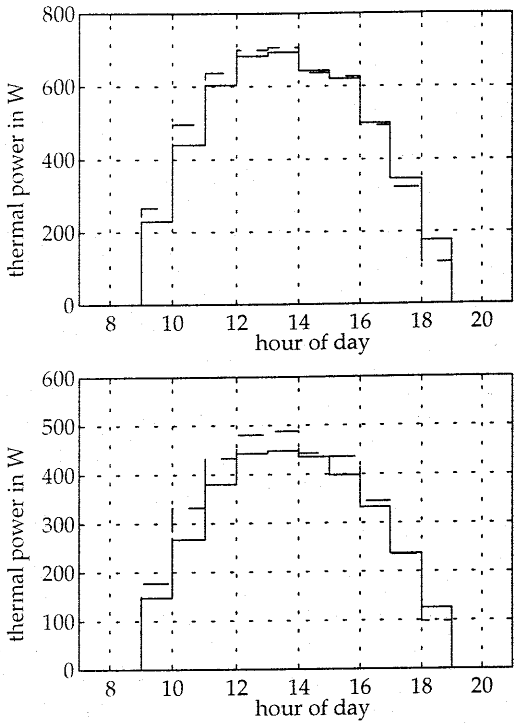

Fig. 10. Calculated (dashed) and measured (solid) thermal power for the conventional thermal collector (above) and the combi-panel (below), on July 12, 1997, against the hour.

The results of the simulation are presented in figures 10-12. Figure 10 shows a good correspondence between the measurements and the simulations, although the calculated values tend to be slightly larger than the measured values, as found before. In addition, it can be observed that the simulations somewhat over predict the measured thermal efficiency in the morning and slightly under predict the measured thermal efficiency in the evening. It was found that this was due to the effect of the roof tiles, which effectively increased the heat capacity of the system. These results indicate that the assumption of thermal equilibrium in the simulations works quite well. On the basis of these results, it is concluded that hourly data are sufficiently accurate to give a good estimate of the annual thermal yield of the system, especially since the effect of the roof tiles largely cancels over a day.

Figure 11 shows the electrical power of the system and figure 12 shows the temperature difference between the PV-panel and the combi-laminate. Figure 11 indicates that the electrical efficiency of the PV-laminate and the PV/T collector are almost the same. At the other hand, figure 12 indicates that in the PV/T-unit the temperature of the PV is much lower than the temperature of the conventional PV unit for the present case in which the inlet temperature was kept constant at approximately 18 ^{0}C. This implies that the electrical gains due to cooling of the PV by the water are of the same order as the optical loss of the PV/T-collector, that is due to the reflection at the glass cover.

4.2 Annual Yield

Next, simulations were performed to find the thermal and electrical yield of the prototype combi-panel for the Dutch KNMI test reference year. The program was used to model the

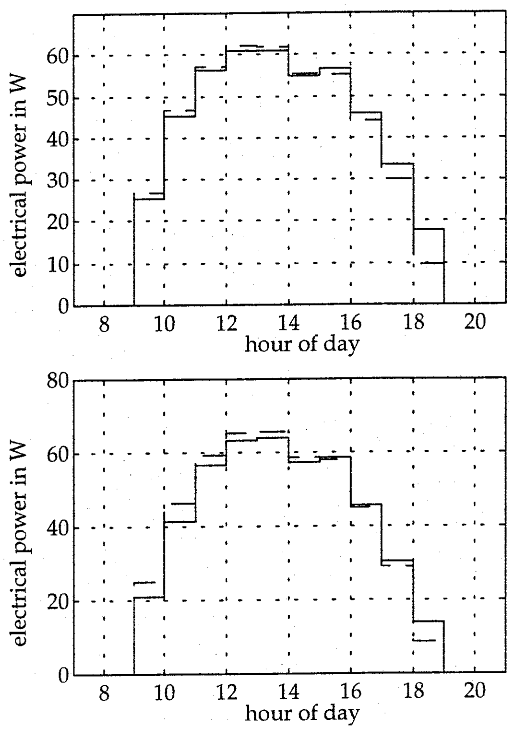

Fig. 11. Calculated (dashed) and measured (solid) electrical power for the PV-panel (above) and for the combi panel (below), on July 12, 1997, against the hour.

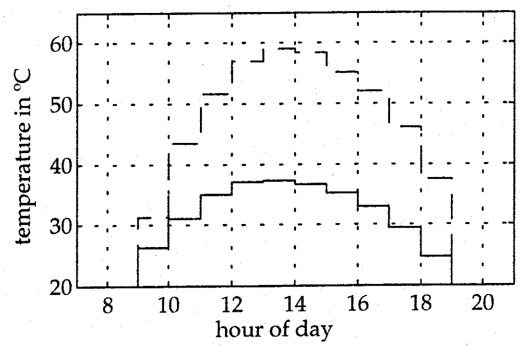

Fig. 12. Measured temperature of the PV panel (dashed) and the PV/T-laminate (solid), on July 12, 1997, against the hour.

case in which two similar combi-panels with a joined area of 3.5 m^2 and a mass flow of 50 kg/(m^2 hr) were used to heat a container of 175 litres of water from 10 ^{0}C up to 60 ^{0}C. A boiler unit was assumed to do the remainder of the heating required if a temperature level of 60 ^{0}C could not be reached by the PV/T unit. The tapping pattern was modelled after the hot water withdrawal schedule of the ISSO (Institute for Study and Stimulation of Research in the area of heating and air conditioning), which is presented in table 1.

The thermal and electrical efficiencies were found to be 33% and 6.7% for the configuration used, as compared to 54% for the conventional thermal collector and 7.2% for the conventional PV-laminate under the same conditions. The electrical efficiency was calculated from an efficiency of the PV-laminate of 9.7% at 25 ^{0}C, corresponding to figure 4, and an inverter efficiency of typically 92%. Due to reflection of 8% of the incoming light at the glass cover, a thermal efficiency of $0.92 \times 7.2\% = 6.6\%$ would be expected if the temperature effect on the PV could be ignored. This implies an increase in electrical efficiency of 0.1% of the yearly electrical efficiency due to the temperature effect. Clearly, for the yearly electrical efficiency, the effect of the glass cover is much more important than the effect of the temperature, which largely cancels out over the year. However, if the present collector would have been used for a low-temperature system instead of for the production of hot tap water, the increase in electrical efficiency due to the temperature effect would have been larger, as indicated by the results presented in figures 11 and 12.

Finally, the annual thermal and electrical efficiencies were calculated when the special features of the combi-panel were successively removed. The results are summarised in table 2.

Configuration	**Annual thermal efficiency**	**Annual electrical efficiency**
Annual thermal efficiency of the combi-collector	33.4%	6.7%
Optical efficiency increased	41.0%	6.5%
Heat resistance removed	44.7%	6.7%
Emission factor reduced	49.9%	6.6%
Additional heat transfer sideways	49.6%	6.6%
No electricity production	54.4%	0%

TABLE 2. Contribution of the various loss mechanisms in the annual electrical efficiency of the combi panel.

This table shows that the thermal loss due to production of energy is smaller than the electrical gain. This is due to the fact that the PV is effectively cooling the system by converting irradiation to electricity instead of heat. This implies a small reduction in thermal losses. The thermal loss due to production of electricity is only 5%, whereas the electrical energy produced amounts to 6.7% of the yearly irradiation.

5 CONCLUSIONS

A non-optimised first prototype of a combi-collector was built. From the measurements the thermal efficiency at zero reduced temperature in the absence of the production of electricity was found to be 59%, which is 25% less than the thermal efficiency found for the corresponding thermal collector. The electrical efficiency with electricity production was found to be 54% and the corresponding electrical yield is around 8.3%. From the KNMI test reference year and the ISSO tapping schedule, an annual efficiency of 33% thermal and 6.7% electrical was found if the collector was employed in a domestic water heating system.

From the simulations, the magnitude of the factors limiting the performance of the combi-panel can be determined. The reduction in the annual electrical efficiency is mainly due to reflection at the insulating glass cover on top of the thermal collector (approximately 0.6% absolute). The reduction in thermal efficiency of the panel is mainly due to the fact that the glass on top of the PV-laminate is not spectrally selective which increases radiation losses (5% absolute) and the fact that the absorption of the PV-laminate is lower than the absorption of the thermal collector due to reflections in the PV-laminate (8% absolute).

This model has proven to be an important tool for further optimisation of the combi-panel. The results were used to build an improved prototype of the combi panel, which is presently under study.

REFERENCES

Duffie J.A. and Beckman W.A. (1991*) Solar Rngineering of Thermal Processes*, 2nd edn, Wiley Interscience, New York.

Vries D.W. de, Helden W.G.J. van, Smulders P.T., Steenhoven A.A. van, and Zolingen R.J.C. van (1997). Design of a Photovoltaic/Thermal combi panel momentary output model, outdoor experiment, *ISES 1997 Solar World Congress, August 24-30 Taejon Korea.*

Vries D.W. de (1998), Design of a PV/Thermal Combi Panel, *PhD Thesis Eindhoven University of Technology.*

Vries D.W. de, Steenhoven A.A. van, Helden W.G.J. van, and Zolingen R.J.C. van, (1999) A panel-shaped, hybrid photovoltaic/ thermal device, *Dutch Patent 1006838.*

Hour	1	2	3	4	5	6	7	8	9	10	11	12	13	14	15	16	17	18	19	20	21	22	23	24
Tapping	-	-	-	-	-	-	-	+	-	-	-	-	+	+	-	-	-	+	+	+	-	+	+	-

TABLE 1. ISSO warm water withdrawal schedule, (-) no withdrawal, (+) 175/8 litres withdrawal.